Vision-based Extraction of Geometry and Forces from Fabricated Micro Devices

Xiaoye Wang, G. K. Ananthasuresh, and James P. Ostrowski

Mechanical Engineering and Applied Mechanics, University of Pennsylvania
220 S. 33rd Street, Philadelphia, PA 19104-6315, {xiaoyew, gksuresh, jpo}@seas.upenn.edu

ABSTRACT

In the field of micro-electromechanical systems (MEMS), there are often times when a model derived directly from the microstructure of a fabricated device would be useful. In our research, the image of the structure is taken by a CCD camera mounted on a microscope. This image is then processed to get the basic physical features on which a physical model can be established. This model can then be used for further analysis and simulation. We present some examples of generating both a CAD solid model and a macro-scale-manufactured prototype. In addition, we are studying the ability to use such visual measurements in order to determine deformations, strains, and forces present in a deformable structure under loading. This is done using images of the original and deformed structure to determine the deformation gradient, and from this solving an inverse problem to find the external loading. Our methodology and the numerical difficulties encountered in this approach will be discussed.

Keywords: CAD/CAE/CAM, computer vision, force recovery.

1 INTRODUCTION

The exact geometry of fabricated MEMS devices is necessary and sometimes critical for accurate simulation and theoretical characterization. A cantilever beam built in a surface micromachining process is known to exhibit markedly different electrostatic pull-in behavior if the exact geometry of the compliant support and any over-etch in the process are not modeled well [1, 2]. It is not always possible to foresee these features to incorporate them when creating solid models from mask designs and process data alone. For a range of MEMS devices from a simple cantilever to a complex wedge motor [3] and several microfluidic devices, it is helpful to be able to create geometric models directly from the manufactured micro prototypes. This procedure, called *reverse engineering for MEMS,* is discussed in this paper along with two applications. The first application is using scaled-up macro prototypes for evaluation and re-design of MEMS and the second, the feasibility of a non-contact, vision-based force sensor for micro devices. The reverse engineering technique for MEMS and the two applications are discussed briefly in the following sections. For details, see [4].

2 GEOMETRY EXTRACTION

The reverse engineering procedure is illustrated in Figure 1. First, a digital image is captured using a CCD camera mounted on a microscope for 2-D top-view extraction. Using various image processing algorithms [5, 6] and data conversion techniques, the following operations are carried out: (i) binary thresholding (ii) edge detection (iii) edge chaining (iv) curve fitting to generate planar models based on lines and circular arcs (v) conversion to IGES format (vi) exporting into any commercial solid model software to build an extruded 3-D model.

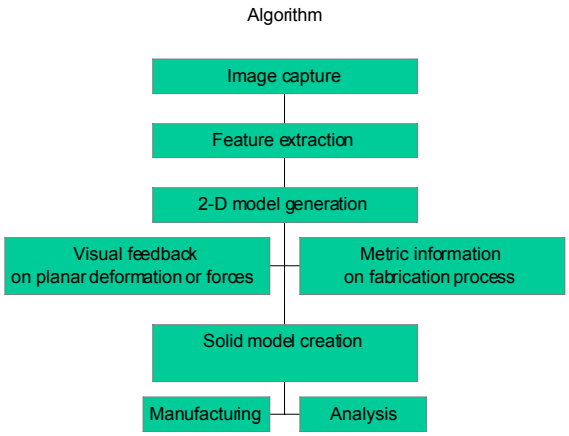

Figure 1: Reverse engineering for MEMS.

Edge detection: First, we convert the captured gray scale image to a binary (black and white) image by choosing a suitable threshold. We have developed an algorithm to extract the pixels that form the edges in the binary image.

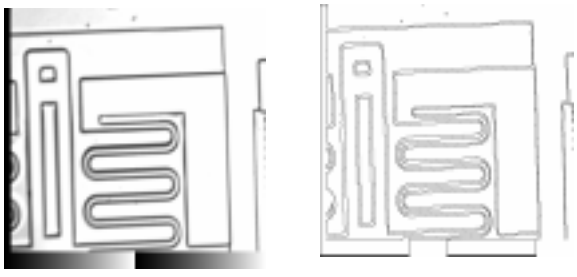

a) Original image b) Obtained edge

Figure 2: Edge detection.

Chaining: In this step, we further examine the collection of pixels that form the edges to group them separately in order to identify closed or open curves. Each closed or open curve is formed by chaining the pixels using an efficient edge-chaining algorithm. The location of each pixel is used to denote the coordinates of each point on the curves.

Arc and line extraction: Curves formed by chaining the edge-points are not in a compact format to export to a standard solid modeling software. Therefore, we fit circular arcs and straight lines to the edge-pixels. We first fit circular arcs to the data wherever possible within the specified accuracy using a least square algorithm. We use the remaining edge-points to fit straight lines. The essential information regarding the arcs and lines is written in the IGES format.

Solid model creation: Based on the extracted arcs and lines, an IGES file is written. We have chosen to use the IGES format because it is compatible with many different modeling analysis software packages. Finally, by extrusion a 3-D model can be obtained, for example, in ProEngineer [7]. Since we have a single image (a projection), only an extruded model can be built. If multiple images from different viewpoints are used, a more accurate 3-D model could be reconstructed. The following (Figure 3) is the 3-D model we created for a silicon device, in this case a micro-gripper where exact profile with all its imperfections is reflected in the solid model. SEMs that provide the perspective views, taken from multiple directions will be necessary to replicate 3-D features.

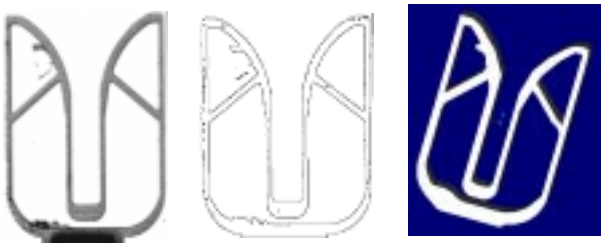

a) Original image b) Extracted edge c) 3-D model

Figure 3: 3-D model reconstruction.

3 MACRO PROTOTYPES FOR MEMS

Just as scaled-down models are used for testing and evaluation of massive objects such as aircraft and ships before manufacturing prototypes of actual size, in MEMS too there are situations when a scaled-up prototype is useful and economical in the design stage. It should be noted however that many transduction processes used in MEMS (for example, electrostatic force) couldn't easily be replicated at macro scale. Macro prototypes are especially useful in purely mechanical MEMS where intermittent contacts occur among the rigid and compliant elements and require accurate dynamic simulation.

Once a 3-D model is generated, we can generate a macro-scale prototype. This can be done in many different ways, e.g.; CNC machining, stereolithography, fused deposition modeling (FDM), etc. From the macro-scale model, we can learn more about the device. Moreover it provides a good means for visualization and manipulation of the microstructure. In ProEngineer, an "stl" file could be output from the 3-D model. Then an ABS plastic model (macro-scale) can be made by an FDM1650 stratasys rapid prototyping machine. Figure 4a is the FDM model we made based on the 3-D model. Figure 4b shows the wedge-motor made using Sandia's SUMMiT process [3]. Using the mask data and process information, we created and tested a macro prototype of the micro wedge-motor.

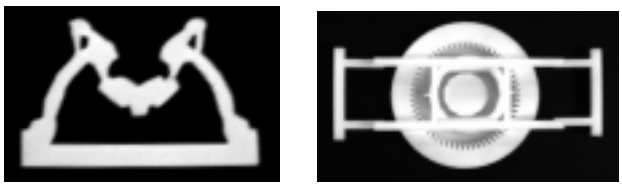

a) Gripper b) Wedge motor

Figure 4: ABS plastic macro models.

4 FORCE RECOVERY

Using visual measurements of a deformable micromechanical structure before and after application of the force, we compute the forces by solving an inverse nonlinear elastic analysis problem. From prior and subsequent geometric profiles, using a discretized finite element model, Cauchy-Green deformation gradient and from this nonlinear logarithmic strain filed are computed. Knowing constitutive properties of the material, the stress field and then internal forces for each element are obtained. Summing up internal force contributions from all elements at a node, the external forces and support reactions are obtained. This forms the basis for our vision-based force sensor for MEMS.

4.1 Finite element model

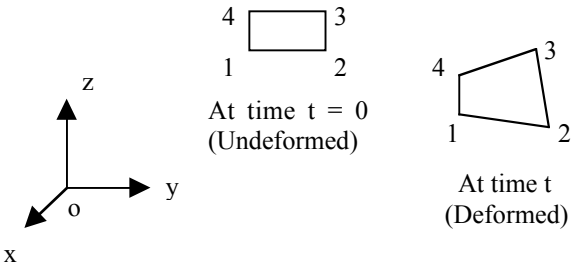

Figure 5: Isoparametric finite element model.

Planar isoparametric finite elements are adopted in our model (Figure 5). We first compute the deformation gradient from the displacement field. Using the deformation gradient, we compute the strain in each element. The deformation gradient matrix is defined as below.

$$X = \begin{bmatrix} \frac{\partial {}^t x}{\partial {}^0 x} & \frac{\partial {}^t x}{\partial {}^0 y} \\ \frac{\partial {}^t y}{\partial {}^0 x} & \frac{\partial {}^t y}{\partial {}^0 y} \end{bmatrix} \quad (1)$$

Where X is the deformation gradient matrix; ${}^t x$, ${}^t y$ are the coordinates of the deformed structure; and ${}^0 x$, ${}^0 y$ are the coordinates of the undeformed one.

There are several large strain measures [8] we can choose from. In our research, the logarithm strain is chosen since it corresponds to the true stress. The logarithm strain can be computed from the formulae given below:

$$C = X * X^T \quad (2a)$$

$$V = C^{1/2} \quad (2b)$$

$$\varepsilon = \ln(V) \quad (2c)$$

Where ε is the logarithm strain.

By knowing the material properties, the stress can be obtained from the strain. Here we assume the material is still linear even though the strain could be large. For the 2-D plane-stress problem, the material property matrix is defined as:

$$M = \frac{E}{1-\nu^2} \begin{bmatrix} 1 & \nu & 0 \\ \nu & 1 & 0 \\ 0 & 0 & (1-\nu)/2 \end{bmatrix} \quad (3)$$

Where E is Young's modulus and ν is Poisson's ratio. Then the stress, σ, can be obtained simply from the strain, ε, as:

$$\sigma = M * \varepsilon \quad (4)$$

Where σ is the stress and ε is the strain.

For each finite element, the internal force can be computed from the following formula:

$$B = \frac{f\varepsilon}{fq} \quad (5)$$

$$F = \int B^T \sigma dV \quad (6)$$

Where ε is the strain; q is the displacement; σ is the stress; and F is the internal force vector. We use a numerical method to evaluate the B matrix in the above formula. Gauss quadrature points are taken to evaluate the integration. Figure 6 shows the Gauss points for 4-node element and 8-node element (the cross marks are Gauss points).

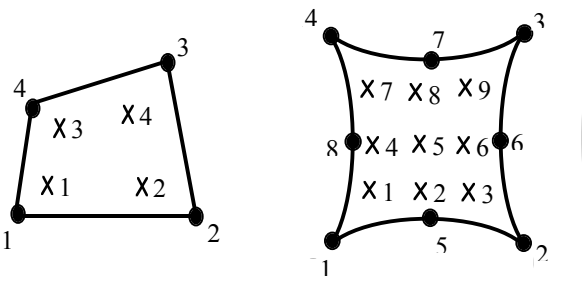

a) 4-node element b) 8-node element

Figure 6: Gauss points in the element.

Once the internal forces for each element are computed, by summing up the internal forces at the common nodes, we can obtain the applied load at each nodal point.

4.2 Numerical Simulation

In this section, we investigate the ability to solve this inverse problem using the method described above. A numerical simulation is performed on the compliant crimping mechanism using ABAQUS [9]. Due to device symmetry, we show only the upper half of the device. The deformation due to the tip load (at the right) was first solved in ABAQUS. Based on this deformation, the force was recovered. The following figures show the force recovery from initial and final deformations. The arrows indicate recovered forces. In Figure 7a, the extreme left nodes and bottom nodes are constrained in both x and y directions which is the large displacement and large strain case. In this case, the force recovery is accurate and the support reaction forces and the external force are clearly seen. In Figure 7b, the extreme left nodes are fixed in both directions, but the bottom nodes are just constrained in the y direction, which is the large displacement and small strain case. In this case, the recovery is not good and some "unnecessary" nodal forces appear because strains are too small and are affected by numerical errors. We discuss these issues further below.

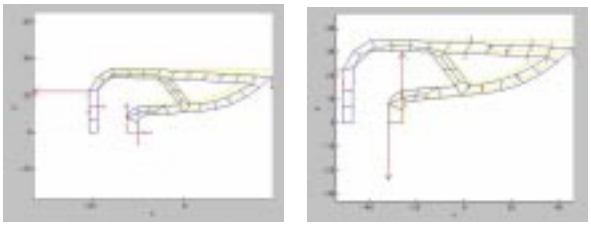

a) Large strain case b) Small strain case

Figure 7: Simulation result.

A theoretical sensitivity analysis shows that the strain computation is very sensitive to the perturbation in the displacement field.

Let the left Cauchy-Green symmetric matrix C defined in Equation 2a be written in the following form.

$$C = \begin{bmatrix} c_1 & c_2 \\ c_2 & c_3 \end{bmatrix} \tag{7}$$

We define the sensitivity of the relative error for ε_{ij} defined in Equation 2c with respect to c_k as follows.

$$S_{ij,k} = \frac{f\varepsilon_{ij} / \varepsilon_{ij}}{fc_k / c_k} \tag{8}$$

Sensitivity analysis shows $S_{11,1}$ and $S_{22,3}$ will approach infinity when the strain is very small. See [4] for details.

4.3 Experimental results

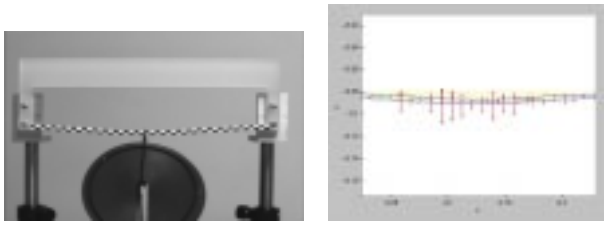

a) Deformed macro-beam b) Vision based load recovery

Figure 8: Experiment on the macro-beam.

Experiment on the macro-beam: A simple experiment has been done on a fixed-fixed polypropylene beam ($206mm \leftarrow 4mm \leftarrow 6mm$). Figure 8a shows the experimental setup. A CCD camera is used to capture the images of the undeformed and deformed shape of the experimental object. Black and white checkerboard pattern was pasted on the beam in order to identify the mesh points. The recovered forces are shown as the arrows in Figure 8b. However, except for the expected external load, a lot of "unnecessary" forces that are originated from the experimental displacement error are observed. This is because the force recovery is sensitive to the displacement, which means unless the precise displacements are obtained, we are unable to recover the load accurately. One way to improve this is to magnify the image in order to reduce the error. But generally, a single visual measurement is not a proper approach to get the accurate displacement field.

Experiment on the micro-beam: Since a lot of MEMS system can be modeled as the frame, a Matlab code for 2-D nonlinear finite element analysis based on the frame element was developed. By solving the forward problem iteratively, we can recover the applied load. Figure 9 shows the algorithm we used to recover the single force.

A micro steel beam ($800\mu m \leftarrow 21\mu m \leftarrow 25\mu m$) is made for the experimental use. The beam is fixed at both ends and a force is applied in the middle as shown in Figure 10. Using the algorithm provided above, we can recover the applied load as 0.1657 (N).

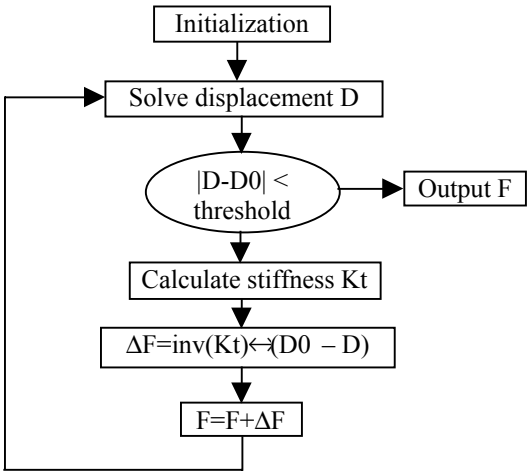

Figure 9: The flow-chart for the force recovery.

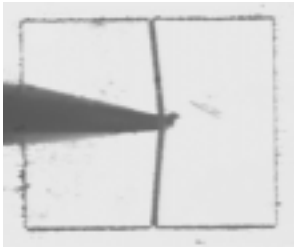

Figure 10: Deformed micro beam.

REFERENCES

[1] G. K. Ananthasuresh and S. Kota, "Mechanical Design Issues in MEMS," CD-ROM proc. of 1997 ASME Design Automation Conference, Irvine, CA.

[2] R. K. Gupta, E. S. Hung, Y.-J. Yang, G. K. Ananthasuresh, and S. D. Senturia, "Pull-in Dynamics of Electrostatically-Actuated Beams", 1996 Solid-State Sensor and Actuator Workshop, Late News, Hilton Head, SC, June 1996.

[3] J. Allen, Sandia National Laboratories, "Mask and process data of a wedge micro motor," private communication.

[4] X. Wang, G. K. Ananthasuresh, and J. P. Ostrowski, "Vision-based Extraction of Forces from Fabricated Micro Devices," manuscript in preparation for *Finite Elements in Engineering* journal.

[5] V.S. Nalwa, "Edgel aggregation and edge description", Computer vision, graphics, and image processing, Vol. 40, No.1, October, pp. 79-94, 1987.

[6] Scott E Umbaugh, "Computer Vision and Image Processing," 1998.

[7] ProEngineer, Parametric Technology Corp., www.ptc.com.

[8] J. Bonet and R. D. Wood, "Nonlinear continuum mechanics for finite element analysis", Cambridge University Press, 1997.

[9] Hibbit, Karlsson, and Sorensen, "Abaqus/Theory Manual," ver.5.8, 1998.